A 69-year-old man with generalised lymphadenopathy, glandular swelling and pleural effusion

Shan Kai Ing [1], Yih Hoong Lee[1], Nga Hung Ngu[1], Kelly Kee Yung Wong[2], Adam Malik bin Ismail[3], Chan Sin Chai[4], Siew Teck Tie[4] and Sze Shyang Kho [4]

[1]Division of Respiratory, Department of Medicine, Sibu General Hospital, Ministry of Health, Sibu, Sarawak, Malaysia. [2]Department of Radiology, Sibu General Hospital, Ministry of Health, Sibu, Sarawak, Malaysia. [3]Department of Pathology, Sarawak General Hospital, Ministry of Health Malaysia, Kuching, Sarawak, Malaysia. [4]Division of Respiratory, Department of Medicine, Sarawak General Hospital, Ministry of Health Malaysia, Kuching, Sarawak, Malaysia.

Corresponding author: Shan Kai Ing (shankai1992@gmail.com)

Shareable abstract (@ERSpublications)
Patients with multisystemic presentation including respiratory symptoms and generalised lymphadenopathy should alert the clinician to this potential diagnosis https://bit.ly/4eJ0PHT

Cite this article as: Ing SK, Lee YH, Ngu NH, *et al*. A 69-year-old man with generalised lymphadenopathy, glandular swelling and pleural effusion. *Breathe* 2025; 21: 240125 [DOI: 10.1183/20734735.0125-2024].

Received: 23 June 2024
Accepted: 28 Sept 2024

A 69-year-old Southeast Asian male presented to our healthcare facility with a 5-month history of persistent nonproductive cough accompanied by loss of appetite and substantial weight loss, amounting to approximately 20 kg. He reported the presence of multiple slowly enlarging, painless neck lumps. He did not experience any sicca symptoms, fever, pruritus, haemoptysis, fatigue, dyspnoea, drenching night sweats or chest pain. Notably, his medical history included dyslipidaemia and ischaemic heart disease without any family or personal history of malignancy. He is a former cigarette smoker who consumed 0.1 pack-years' worth of cigarettes and stopped smoking 40 years ago. He occasionally consumes alcohol during festive events. The patient had an allergy to trimethoprim/sulfamethoxazole, and his past surgical history included a laparoscopic cholecystectomy for gallstone disease. Professionally, he worked as an administrative executive in a government department. Outside of work, he did not have any special hobbies or interests. He maintained a responsible lifestyle that was free of high-risk behaviours.

Upon physical examination, the patient was thin, weighed 38 kg, and had a body mass index (BMI) of 16 $kg \cdot m^{-2}$. The patient was afebrile, with a heart rate of 108 beats per min and blood pressure of 136/68 mmHg. The patient's respiratory rate and oxygen saturation levels were within normal limits. Multiple soft, painless swellings measuring approximately 3 cm×5 cm were palpable over the bilateral submandibular region. In addition, there were multiple matted, rubbery, painless swellings over the bilateral cervical region. Upon examination of the lungs, reduced breath sounds were noted over the bilateral lower zones, without any added sounds. Abdominal examination revealed no hepatosplenomegaly. Other systemic examinations revealed no remarkable findings.

Table 1 shows the results of the laboratory investigations, which in summary revealed normochromic normocytic anaemia, eosinophilia, thrombocytosis, hyperglobulinaemia, increased erythrocyte sedimentation rate and raised immunoglobulin E level. The patient's bloodborne virus screening test results were negative, and a polyclonal increase in gamma globulin was detected with a negative urine paraprotein level. Notably, serum complement levels were low. The tuberculosis workups were negative, and the comprehensive autoimmune workups yielded negative results.

Plain chest radiography demonstrated a blunted right costophrenic angle. A contrast-enhanced computed tomography (CT) followed by ^{18}F-fluorodeoxyglucose positron emission tomography (^{18}F-FDG/PET) CT was arranged to further evaluate the extent of lymphadenopathy and involvement of other organs.

TABLE 1 Laboratory investigations

Test	Result	Normal range
Haemoglobin, g·dL^{-1}	9.8	12.0–15.0
White blood cell, ×10^{3}·mm^{-3}	7.0	4.0–10.0
Neutrophil count, ×10^{9}·L^{-1}	4.0	2.0–7.0
Lymphocyte count, ×10^{3}·mm^{-3}	1.9	1.0–3.0
Eosinophil count, cells·µL^{-1}	700	20–500
Platelet, ×10^{3}·mm^{-3}	816	150–410
Serum globulin, g·L^{-1}	108	20–35
Erythrocyte sedimentation rate, mm·h^{-1}	140	1–10
C-reactive protein, mg·L^{-1}	1.8	<10
Immunoglobulin E, kU·L^{-1}	1489	Up to 160
Complements level, g·L^{-1}		
C3c	0.62	0.90–1.80
C4	0.15	0.10–0.40
Serum protein electrophoresis, g·L^{-1}		
Total	131	60–80
Gamma	92.1	4.8–12.6
24-h urine protein, g	0.56	<0.15
Tumour markers		
Carcinoembryonic antigen (CEA), ng·mL^{-1}	1.9	<5.0
Cancer antigen 19.9 (CA-19.9), IU·mL^{-1}	0.6	<37.0
Alpha fetoprotein (AFP), IU·mL^{-1}	1.6	<15.0
Prostate-specific antigen (PSA), ng·mL^{-1}	0.53	<3.50
Bloodborne virus screening		
Hepatitis B	Non-reactive	
Hepatitis C	Non-reactive	
HIV	Non-reactive	
Antinuclear and extractable nuclear antigen	Negative	
Vasculitis panel		
Anti-MPO	Negative	
Anti-PR3	Negative	
c-ANCA	Negative	
p-ANCA	Negative	
Rheumatoid factor	Negative	
Interferon-γ release assay	Negative	
Sputum for *Mycobacterium tuberculosis* culture	No growth	

Task 1

What does the CT and ^{18}F-FDG/PET CT show (figure 1)?

Go to Answers >>

The contrast-enhanced CT scan also revealed enlarged bilateral lacrimal glands, while ^{18}F-FDG/PET CT demonstrated nodal hypermetabolism at the bilateral cervical level 2, 3 and right supraclavicular nodes, as well as multiple hilar and mediastinal nodal hypermetabolism. Multiple nodal hypermetabolisms associated with mild diffuse omental and mesenteric hypermetabolism were also detected in the abdomen (highest SUV_{max} 4.50, at the right external iliac nodes). Mild splenic hypermetabolism (delayed SUV_{max} 3.72) was observed while no hypermetabolism was detected in the pancreas or liver.

Task 2

What is the provisional diagnosis for this patient at this point in time?

Go to Answers >>

Task 3

What is the next appropriate course of investigation for this patient?

Go to Answers >>

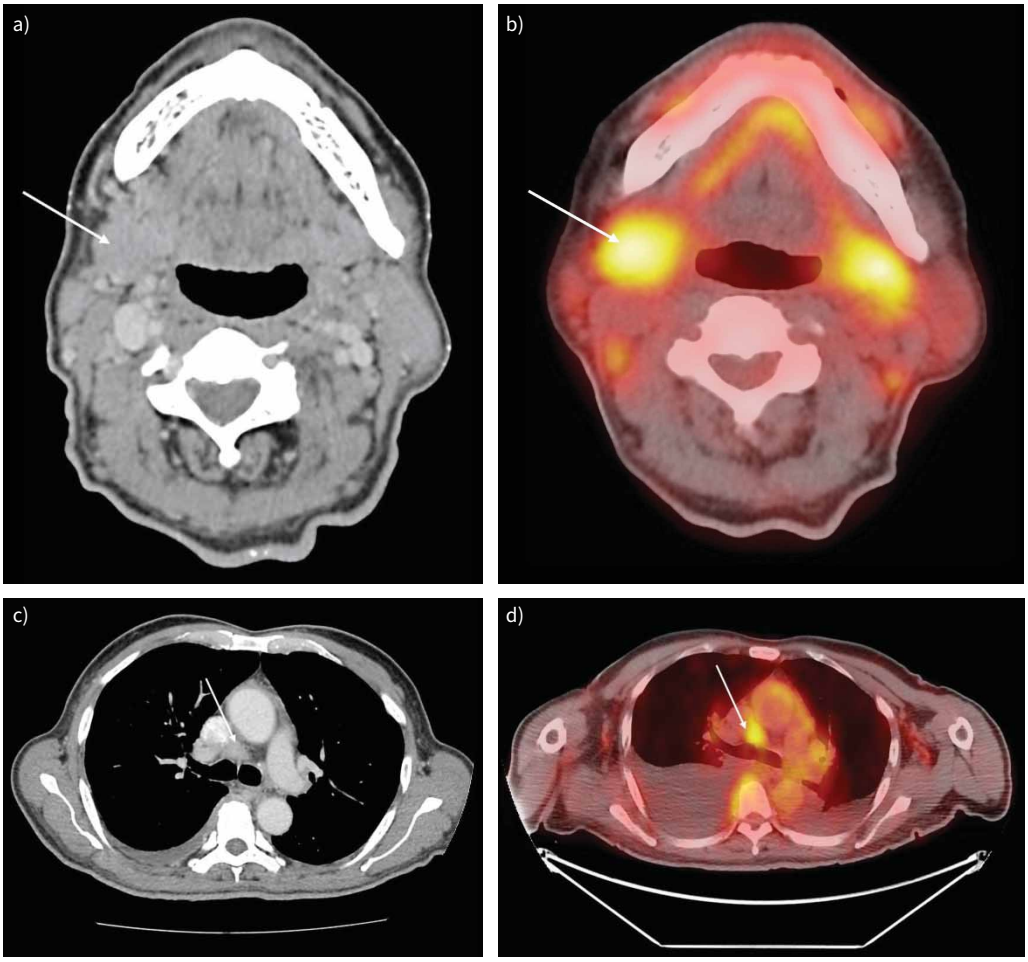

FIGURE 1 Computed tomography (CT) scan and ^{18}F-fluorodeoxyglucose positron emission tomography (^{18}F-FDG/PET) CT of a, b) the submandibular glands and c, d) at the level of pre-carina region.

Otolaryngologists performed multiple excisional biopsies of the cervical lumps to obtain a histopathological diagnosis. However, these biopsies only revealed persistent sialadenitis. Diagnostic right thoracentesis was performed in the primary referring centre and the pleural fluid cytology showed dense lymphocytic infiltration with no atypical cells seen. Additionally, the acid-fast bacilli stained direct smear of the pleural fluid was found to be negative, and the *Mycobacterium tuberculosis* culture returned negative results.

The patient was then referred to the surgical department for further workup, and an upper gastrointestinal endoscopy revealed no abnormalities, while the colonoscopy exhibited pan-diverticulitis. Subsequently, further excisional biopsy of the FDG-avid PET/CT inguinal lymph node showed no evidence of malignancy or tuberculosis. A repeat naso-endoscopy by an otolaryngologist showed thickened mucosa over the left posterolateral oropharynx. Biopsies of the bilateral Fossa of Rosenmüller and thickened left posterolateral oropharyngeal mucosa were performed, but were negative for granulomatous inflammation and malignancy.

Task 4

What is the next best option to obtain tissue diagnosis for this patient?

Go to Answers >>

Owing to inconclusive results and a diagnostic dilemma, the patient was referred to the pulmonology team for consideration of a further biopsy – either a pleural or mediastinal lymph node biopsy. However, a repeat

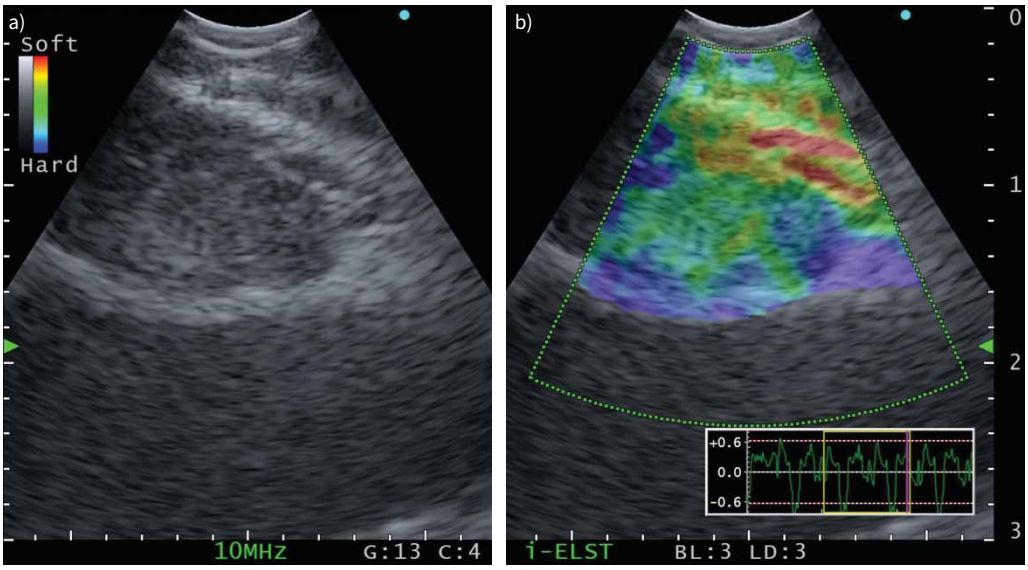

FIGURE 2 Endobronchial ultrasound (EBUS) examination revealed an oval shaped, distinct lymph node at pre-carinal station 4R (a) with intermediate stiffness on elastography assessment (b).

plain chest radiograph and thoracic ultrasound now confirmed resolution of the pleural effusion, which it is not feasible for medical thoracoscopy. After a comprehensive assessment, review and discussion, our team arrived at provisional diagnoses that included IgG4-RD, tuberculous lymphadenitis and lymphoma. Given the patient's ^{18}F-FDG PET/CT scan findings indicating enlarged FDG-avid station 4R and 7 mediastinal lymph nodes, we recommended that the patient to undergo EBUS-TBNA for mediastinal lymph node biopsy. Nevertheless, considering the high clinical suspicion of a rare diagnosis and the unavailability of rapid on-site evaluation (ROSE) in our setting, we suggested concurrent histological sampling through transbronchial mediastinal cryobiopsy (TBMC). The patient has agreed to proceed with EBUS-TBNA and TBMC to allow additional tissue sampling for comprehensive histological analysis.

Under total intravenous anaesthesia, the patient's airway was secured with a laryngeal mask airway. Initial bronchoscopic examination revealed a normal airway. EBUS examination (BF-UC190F, Olympus Medical) then confirmed multiple enlarged mediastinal and hilar lymph nodes, with the largest at station 4R measuring 15×16 mm in diameter with intermediate stiffness on elastography (figure 2). Standard EBUS TBNA was performed with a 22G needle for a total of three passes (figure 3a). The 1.1 mm cryoprobe (ERBE Elektromedizin, Tubingen) was then placed under direct bronchoscopic vision into the target after track dilatation with a high-frequency needle knife (KD-31C-1, Olympus Medical) (figure 3b). The probe was then activated for 5 s, and the echobronchoscope-cryoprobe was swiftly removed *en bloc* from the patient. A total of three cryo-passes were performed, without complications.

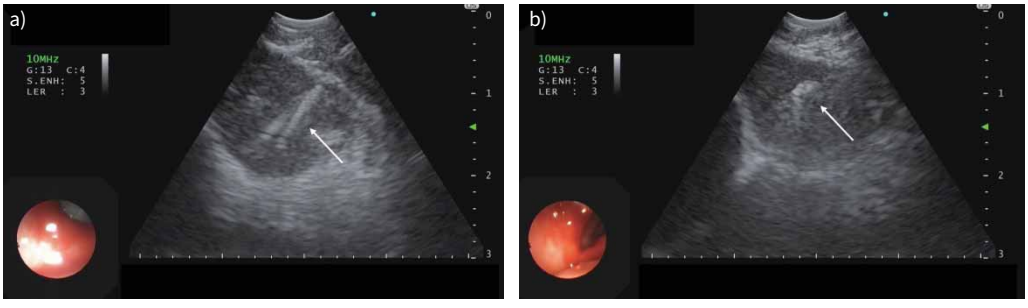

FIGURE 3 Endobronchial ultrasound (EBUS)-guided transbronchial needle aspiration (TBNA) was performed with 22G TBNA needle for three passes (arrow in a), followed by cryobiopsy placing the 1.1 mm cryoprobe into the target lymph node through the track created by TBNA needle and a high-frequency needle knife (arrow in b).

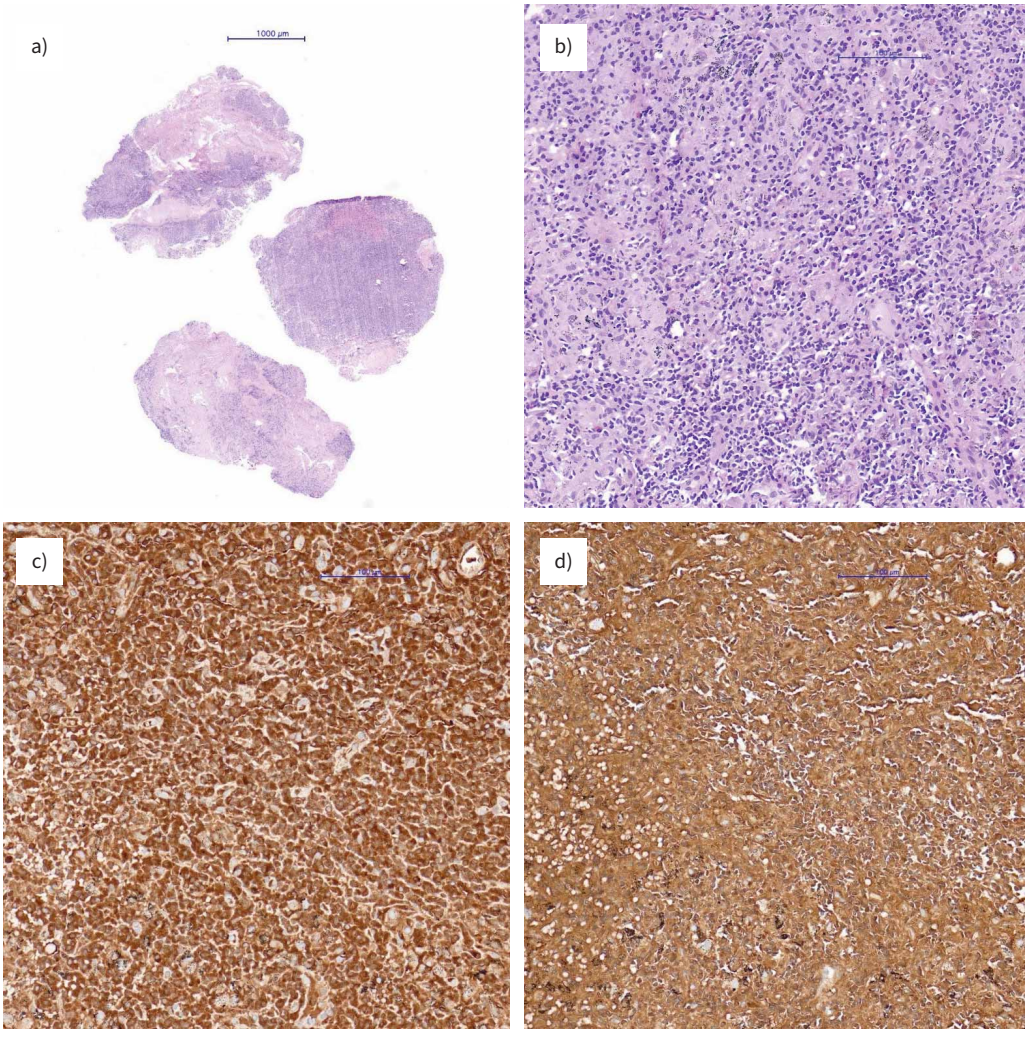

FIGURE 4 a, b) Histopathological analysis of the 4R station cryobiopsy specimens (panel b, ×20 magnification, haematoxylin and eosin stain). c, d) Further specific staining with IgG (panel c, ×20 magnification, IgG stain) and IgG4 (panel d, ×20 magnification, IgG4 stain). Scale bars: a) 1000 µm; b–d) 100 µm.

The cell-block analysis from the TBNA needle biopsy showed only scanty atypical cells mixed with inflammatory and red blood cells. Histopathological analysis of the cryobiopsy tissue measuring 5 mm in total diameter is shown in figure 4a and b. Immunohistochemistry findings ruled out the presence of metastatic carcinomas and lymphomas. The Ziehl–Neelsen and periodic acid-Schiff stains identified no evidence of tuberculous or fungal infection. Further specific staining with IgG and IgG4 was ordered due to our clinical suspicion of IgG4-RD (figure 4c and d).

Task 5

What does the histopathological analysis and IgG/IgG4 staining of the station 4R cryobiopsy specimens show (figure 4a–d)?

Go to Answers >>

Upon re-evaluation of the initial salivary gland biopsy by a thoracic pathologist, storiform fibrosis, obliterative phlebitis, and a high IgG4/IgG staining ratio were observed (figure 5). The total serum IgG level was subsequently evaluated and found to be markedly elevated at 7387 $mg \cdot dL^{-1}$ (normal range 767–1590 $mg \cdot dL^{-1}$), with a specific IgG4 level of 6207.1 $mg \cdot dL^{-1}$ (normal range 2.4–121.0 $mg \cdot dL^{-1}$). These findings supported a final diagnosis of multisystem IgG4-RD.

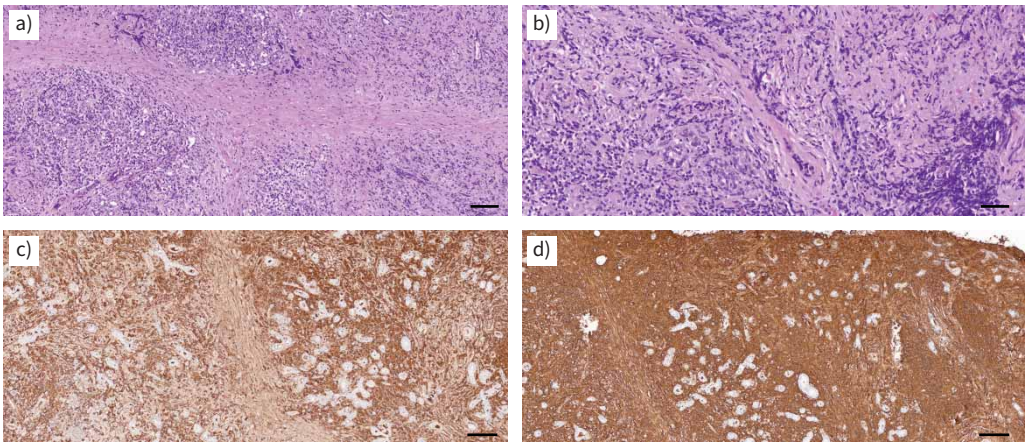

FIGURE 5 Histology of initial salivary gland biopsy revealed storiform fibrosis (panel a, ×10 magnification, haematoxylin and eosin (H&E) stain) and obliterative phlebitis (panel b, ×20 magnification, H&E stain). Staining with IgG (panel c, ×10 magnification, IgG stain) and IgG4 (panel d, ×10 magnification, IgG4 stain) revealed high IgG4/IgG staining ratio. Scale bars: a, c, d) 200 µm; b) 100 µm.

Task 6

What is the best treatment option for this patient?

Go to Answers >>

Following a definitive diagnosis of IgG4-RD, the patient was initiated on oral glucocorticoid therapy with prednisolone at a dose of 40 mg daily (1 $mg \cdot kg^{-1}$). The initial dose of prednisolone was maintained for a period of 4 weeks and then gradually reduced by 10 mg every 2 weeks until reaching a daily dose of 5 mg, with the patient's symptoms and side-effects being closely monitored throughout the process. A nephrologist and rheumatologist were also consulted during his course of treatment.

After administering glucocorticoid therapy for a month, the patient's persistent dry cough symptom has been entirely alleviated. At the end of the 3-month treatment period, the patient experienced significant symptom improvement, including a reduction in glandular swelling, an increase in weight from 38 to 50 kg, and an increase in BMI from 16 $kg \cdot m^{-2}$ to 21 $kg \cdot m^{-2}$. Throughout the treatment, no apparent adverse effects from the glucocorticoid were detected, including hyperglycaemia, psychosis, increased susceptibility to infections, gastritis or myopathy. After 3 months, the CT scan was repeated to assess the treatment response.

Task 7

What does the CT scan show after 3 months of prednisolone (figure 6)?

Go to Answers >>

The patient's serum IgG4 level significantly decreased by 79%, from 6207.1 $mg \cdot dL^{-1}$ to 1301.8 $mg \cdot dL^{-1}$. The dosage of prednisolone was gradually reduced during follow-up, and a steroid-sparing agent was deemed unnecessary as disease remained under control with a daily prednisolone maintenance dose of 5 mg (0.1 $mg \cdot kg^{-1}$).

Discussion

IgG4-RD is an increasingly recognised fibro-inflammatory disorder that can affect multiple organs [2]. It has been previously referred to as IgG4 multiorgan lymphoproliferative syndrome, IgG4 sclerosing disease and IgG4-related systemic plasmacytic syndrome. The Japanese IgG4 research programme team published the first comprehensive diagnostic criteria for IgG-RD in 2011, which have been accepted worldwide. In 2020, the Japanese team updated the revised comprehensive diagnostic criteria for IgG4-RD, which consists of three domains: clinical and radiological features, serological diagnosis, and pathological diagnosis. The new pathological diagnosis includes storiform fibrosis and obliterative phlebitis. Patients with a possible or probable diagnosis by comprehensive diagnostic criteria who fulfill the organ-specific criteria for IgG4-RD, which includes autoimmune pancreatitis, lacrimal gland, saliva adenitis, kidney

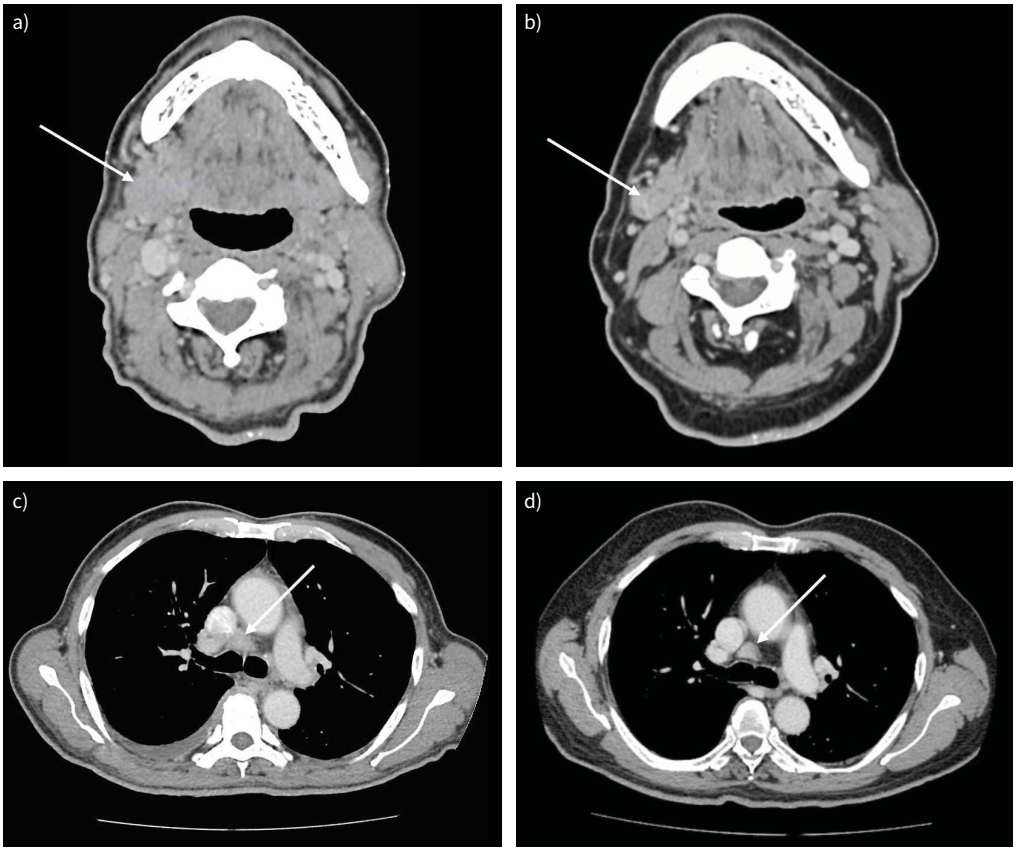

FIGURE 6 3-month surveillance computed tomography (CT) scan at the level of submandibular glands as well as station 4R lymph node. a, c) CT scan on presentation, b, d) 3-month surveillance CT scan.

disease, sclerosing cholangitis, ophthalmic disease, respiratory disease, large periarteritis/periarteritis and retroperitoneal fibrosis, are also classified as having a definite diagnosis of IgG4-RD [3]. However, despite the well-established diagnostic criteria, clinicians may overlook IgG4-RD during clinical diagnosis due to a lack of awareness and exposure to the disease, as demonstrated in our case.

Acknowledging that the absence of elevated IgG4 levels does not rule out IgG4-RD is crucial. Roughly 50% of biopsy-proven, clinically active IgG4-RD patients have IgG4 levels within normal limits; conversely, ∼5% of healthy individuals exhibit elevated IgG4 concentrations [4]. Given this serological variability, histopathological assessment is the cornerstone for diagnosing IgG4-RD. This is especially critical as the differential diagnosis encompasses a broad spectrum of diseases, including other multisystem disorders like sarcoidosis and connective tissue diseases, those with similar clinical and radiological features such as interstitial lung diseases, cancer and lymphoma, and conditions characterised by local and systemic inflammation with elevated IgG4 tissue levels, such as ANCA-associated vasculitis and multicentric Castleman disease [5]. The pathological hallmark of IgG4-RD is dense lymphoplasmacytic infiltrate with IgG4-positive plasma cells, storiform fibrosis, obliterative phlebitis and a variable amount of eosinophils. However, as evidenced in our case, diagnosing IgG4-RD poses a significant challenge due to the nonspecific nature of its morphological features. The initial biopsies were deemed inconclusive but were reaffirmed after a second-look, mainly due to the lack of clinical suspicion for IgG4-RD initially. Therefore, achieving a correct diagnosis hinges on clinical acumen and effective communication between the clinician and the pathologist, as this collaboration is essential in recognising and securing the diagnosis of this rare disease.

Thoracic manifestation of IgG4-RD is by no means rare. In fact, ∼30% of patients suffering from systemic IgG4-RD will exhibit thoracic involvement. Moreover, 10% of patients diagnosed with IgG4-RD will have exclusive thoracic manifestation of the disease. In the thorax, the disease can occur in all regions, with the lung being the most commonly affected area, along with lymphadenopathy, pleurae, and retromediastinum [6]. Clinical manifestations of thoracic IgG4-RD are often nonspecific and may include symptoms such as

cough, chest pain, wheezing and dyspnoea. Laboratory abnormalities observed in patients with thoracic IgG4-RD include eosinophilia, hypocomplementaemia, hypergammaglobulinaemia and elevated immunoglobulin E levels. CT-scan findings can be divided into seven distinct patterns, including nodular, ground-glass opacities, interstitial lung disease and peribronchovascular lesions of the lung, as well as extrapulmonary lesions such as lymph node, pleural and retromediastinal patterns [7]. Clinical suspicions of thoracic involvement in IgG4-RD should be raised if there is the presence of clinical signs, laboratory abnormalities and thoracic imaging findings, as shown in our case.

A substantial percentage of patients diagnosed with thoracic IgG4-RD frequently exhibit mediastinal and/or hilar lymphadenopathy, with estimates ranging between 40% and 90% [8]. Furthermore, ^{18}F-FDG PET/CT imaging has proven to be a valuable tool in revealing additional organ involvement compared with traditional diagnostic methods in patients with IgG4-RD [9]. However, obtaining sufficient tissue for histopathological examination remains a significant challenge from the hilar and mediastinum region. Although EBUS allows minimally invasive access into these difficult regions, the majority of EBUS procedures involve fine needle aspiration or mini-forceps, which only yield cytological samples or suboptimal-quality crushed specimens, respectively, as demonstrated in our case. Recently, advancements in bronchoscopy techniques have led to the development of miniaturised cryoprobes, which allow for the insertion of an ultrathin cryoprobe into the working channel of a standard EBUS echobronchoscope. As a result, EBUS-TBMC has emerged as a promising diagnostic approach for mediastinal and hilar pathologies [10]. Ideally, the use of EBUS-TBNA with ROSE should be the standard approach for mediastinal/hilar lymphadenopathies. However, the availability of ROSE may vary across centres. It is important to note that EBUS-TBNA has a lower diagnostic yield for both lymphoma and benign diseases. A study by Maturu *et al*. [11] proposed EBUS-TBMC as an additional diagnostic step to improve the yield of EBUS-TBNA in cases with inconclusive results from ROSE. In our case, due to the unavailability of ROSE and the clinical suspicion of a rare disease, we proceeded with both EBUS-TBNA and TBMC in the same setting after obtaining the patient's consent. However, it is essential to recognise that a pre-procedure provisional diagnosis remains essential and should be communicated to the pathologist, as this will enable proper staining to be ordered to confirm the diagnosis.

Early recognition of potential organ involvement is vital for effective management and preventing irreversible damage. Timely diagnosis of IgG4-RD can significantly impact the patient's prognosis by averting extensive organ destruction and fibrosis [12]. Steroid therapy remains the primary treatment, with oral prednisone at a dose of 0.5–1 mg·kg^{-1} daily being commonly employed. In cases demonstrating a favourable response, gradual tapering over 3–6 months is typically implemented. For resistant or relapsing cases, additional immunomodulatory medications such as rituximab, azathioprine and mycophenolate can be considered, although the evidence guiding the choice of these treatments in IgG4-RD is not robust [13].

In conclusion, IgG4-RD presents a complex and intriguing challenge among autoimmune disorders. A definite diagnosis of IgG4-RD requires the presence of characteristic histomorphological features, IgG4 immunopositivity, and elevated serum IgG4 levels. Patients who do not meet all these criteria are classified as having a possible or probable diagnosis of IgG4-RD. However, those who fulfill the organ-specific criteria for IgG4-RD are considered to have a definite diagnosis. Therefore, histopathological examination of the suspected organs is essential for accurately diagnosing IgG4-RD. Awareness of this rare condition is crucial in achieving a timely diagnosis and preventing long-term complications. Healthcare providers should always consider the possibility of IgG4-RD in patients with multisystemic presentation, especially when faced with challenging diagnostic cases.

Answer 1

The CT scan revealed an enlarged bilateral submandibular gland (figure 1a, arrow) with hypermetabolic signal (highest maximum standardised uptake value (SUV_{max}) 6.82) on ^{18}F-FDG/PET CT (figure 1b, arrow). The CT scan revealed an enlarged station 4R lymph node at the pre-carinal region (figure 1c, arrow) with hypermetabolic signal (highest SUV_{max} of 4.10) on ^{18}F-FDG/PET CT (figure 1d, arrow), as well as bilateral pleural effusions. There was no distinctive lung parenchymal manifestation of IgG4-related disease (IgG4-RD), such as nodular, ground-glass opacities, interstitial lung disease and peribronchovascular lesions.

<< Go to Task 1

Answer 2

The constellation of findings of generalised lymphadenopathy, glandular swelling and pleural effusion with anaemia, eosinophilia, thrombocytosis, hyperglobulinaemia, hypocomplementaemia, elevated erythrocyte sedimentation rate, and an ^{18}F-FDG/PET CT scan showing hypermetabolism of the lymph nodes and glands raised clinical suspicion of lymphoproliferative disease or disseminated tuberculosis.

<< Go to Task 2

Answer 3

Excisional biopsies of the hypermetabolic glands and lymph nodes to obtain histopathological diagnosis.

<< Go to Task 3

Answer 4

These options are appropriate to obtain further tissue diagnosis:

- Re-examine the previous biopsy
- Mediastinoscopy and biopsy
- Endobronchial ultrasound (EBUS)-guided mediastinal transbronchial needle aspiration (TBNA) and cryobiopsy

<< Go to Task 4

Answer 5

Morphological examination revealed the presence of lymphoid tissue characterised by dense lymphoplasmacytic infiltrates and increased eosinophil counts (figure 4b). Further specific staining with IgG (figure 4c) and IgG4 (figure 4d) revealed an IgG4/IgG ratio of 0.9.

<< Go to Task 5

Answer 6

Steroid therapy with oral prednisone at a dose of 0.5–1 mg·kg^{-1} daily remains the primary treatment [1].

<< Go to Task 6

Answer 7

The 3-month surveillance scan confirmed a significant reduction in the size of the bilateral submandibular salivary glands (arrow, figure 6a (on presentation) *versus* figure 6b (3-month surveillance scan)). The pre-carinal mediastinal lymph node also demonstrated significant regression in size (arrow, figure 6c (on presentation) *versus* figure 6d (3-month surveillance scan)), with no recurrence of pleural effusion.

<< Go to Task 7

Conflict of interest: The authors have nothing to disclose.

References

1 Wallace ZS, Katz G, Hernandez-Barco YG, *et al.* Current and future advances in practice: IgG4-related disease. *Rheumatol Adv Pract* 2024; 8: rkae020.
2 Nizar A-H, Toubi E. IgG4-related disease: case report and literature review. *Auto Immun Highlights* 2015; 6: 7–15.
3 Umehara H, Okazaki K, Kawa S, *et al.* The 2020 revised comprehensive diagnostic (RCD) criteria for IgG4-RD. *Mod Rheumatol* 2021; 31: 529–533.
4 Murata Y, Aoe K, Mimura Y. Pleural effusion related to IgG4. *Curr Opin Pulm Med* 2019; 25: 384–390.
5 Strehl JD, Hartmann A, Agaimy A. Numerous IgG4-positive plasma cells are ubiquitous in diverse localised non-specific chronic inflammatory conditions and need to be distinguished from IgG4-related systemic disorders. *J Clin Pathol* 2011; 64: 237–243.
6 Muller R, Ebbo M, Habert P, *et al.* Thoracic manifestations of IgG4-related disease. *Respirology* 2023; 28: 120–131.
7 Inoue D, Zen Y, Abo H, *et al.* Immunoglobulin G4-related lung disease: CT findings with pathologic correlations. *Radiology* 2009; 251: 260–270.

8 Ryu JH, Sekiguchi H, Yi ES. Pulmonary manifestations of immunoglobulin G4-related sclerosing disease. *Eur Respir J* 2012; 39: 180–186.

9 Zhang J, Chen H, Ma Y, *et al.* Characterizing IgG4-related disease with ^{18}F-FDG PET/CT: a prospective cohort study. *Eur J Nucl Med Mol Imaging* 2014; 41: 1624–1634.

10 Botana-Rial M, Lojo-Rodríguez I, Leiro-Fernández V, *et al.* Is the diagnostic yield of mediastinal lymph node cryobiopsy (cryoEBUS) better for diagnosing mediastinal node involvement compared to endobronchial ultrasound-guided transbronchial needle aspiration (EBUS-TBNA)? A systematic review. *Respir Med* 2023; 218: 107389.

11 Maturu VN, Prasad VP, Vaddepally CR, *et al.* Endobronchial ultrasound-guided mediastinal lymph nodal cryobiopsy in patients with nondiagnostic/inadequate rapid on-site evaluation. *J Bronchol Interv Pulmonol* 2023; 31: 2–12.

12 Stone JH, Zen Y, Deshpande V. IgG4-related disease. *N Engl J Med* 2012; 366: 539–551.

13 Perugino CA, Stone JH. IgG4-related disease: an update on pathophysiology and implications for clinical care. *Nat Rev Rheumatol* 2020; 16: 702–714.